Chapter 1

Introduction

> *"The branch of physics we call 'the physics of the solid state' is, in large measure, the study of defects in crystalline solids and the effects that they have on the properties of these solids. In this it has to be contrasted with the parallel science of crystallography, which studies the arrangements of the atoms themselves."*
>
> *- N.F. Mott*
>
> *The Page - Barber Lectures, 1956*

The aim of this thesis is to describe work done investigating disorder in fluorite based oxides. There exist many compounds whose crystal structure is either that of fluorite or closely resembles this structure. This introduction begins with a description of the crystal structure of the compounds considered and then continues with a discussion of disorder and disorder processes. Indeed, there are many ways in which the order in crystalline solids can be disturbed, such as imperfections in position, composition and electronic state [1]. Since this thesis will be concerned with modelling the predictions of disorder, the introduction therefore provides a rudimentary discussion of the means by which disorder is introduced into a lattice.

1.1 Fluorite Based Oxides

1.1.1 MeO_2 Oxides

The term "fluorite" originates with the mineral CaF_2, which is generally known by the same name. Oxides which adopt the fluorite structure or structures related to fluorite have great and varied technological importance. Of those compounds considered in this thesis, applications range from nuclear fuel for UO_2 to thermal barrier coatings and solid oxide fuel cell components for pyrochlores. Despite the vast difference in applications, the crystal structures of fluorite and pyrochlore compounds are very similar. This thesis then begins with a description of structure.

Pauling formulated a set of rules governing the stability of ionic crystal structures [2,3] (also see [4] for a particularly informative discussion of these rules). The first of these states:

> *A coordinated polyhedron of anions is formed about each cation, the cation - anion distance being determined by the radius sum and ligancy of the cation by the radius ratio.*

This is easier to visualize if ions are thought of as spheres, anions surrounding a single cation. The preferential coordination of anions is dependent on the size of the cation with respect the anionic radius. For example, the minimum radius for a cation coordinated by an octahedron is easily calculated to be 0.414 times the radius of the anion, see Figure 1.1. At this distance ratio, the anions just touch and can therefore move no closer. If the cation is any smaller than this, the Coulomb energy becomes defined by the anion-anion distance (assuming the cation remains in the centre). However, by selecting a structure with a lower coordination number, the minimum possible anion-cation distance is smaller and the Coulomb interaction can be greater. Another way of visualizing this destabilization, is that once the cation is smaller than the minimum size for a given coordination it is no longer "fully coordinated," but has room with which to "rattle" about [5].

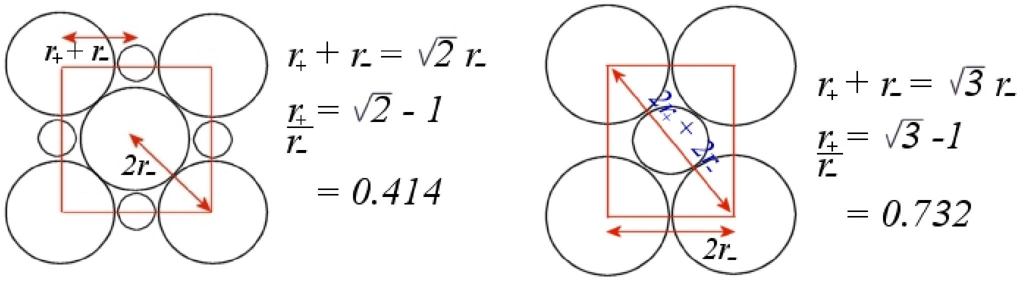

Figure 1.1: The calculation of the radius ratio for octahedral and cubic coordinations.

The cation - anion radius ratio can therefore be used to determine the most stable coordinated polyhedra. Table 1.1 lists the critical ratio values, where the term *"ligancy"* has the same meaning as *"coordination number"* (i.e. the number of atoms bonded to a central atom [2]). In this approach, when the ratio becomes less than any of the critical values given in Table 1.1, the next lower structure becomes preferred.

Polyhedron	Ligancy	Minimum radius ratio	Example Compound
Cubo-octahedron	12	≥ 1.000	none exist
Cube	8	≥ 0.732	CaF_2
Octahedron	6	≥ 0.414	NaCl
Tetrahedron	4	≥ 0.225	ZnS

Table 1.1: The minimum ionic radius ratios for coordinated polyhedra stability, after [2].

Using ThO_2 as an example of a compound crystallizing in the fluorite structure, the ionic radius of 8 fold coordinate Th^{4+} = 1.05Å, while the 4 fold coordinate of

$O^{2-} = 1.38$ Å [6]. Thus, the minimum radius ratio = 0.761, which is considerably above the minimum for a cubic coordination, but still well below the critical value of 1.000 required to form the cubo-octahedron structure. Therefore, Th atoms will be cubically coordinated by O atoms. Th atoms are FCC packed, thus forming a tetrahedron about each O atom and the resulting space group is $Fm\bar{3}m$ [7, 8], see Figure 1.2. Indeed, this description of the fluorite lattice pertains to many other compounds, such as halides (SrF_2), oxides (CeO_2) and intermetallics (NiMgBi). In this work, only oxides are discussed, predominantly UO_2. After examining Figure 1.2, it is clear that there are many unoccupied interstices in the fluorite structure. UO_2 is the most common material used for nuclear fuel [9], in part because of its ability to accommodate fission products in these voids, thereby reducing problematic fuel swelling.

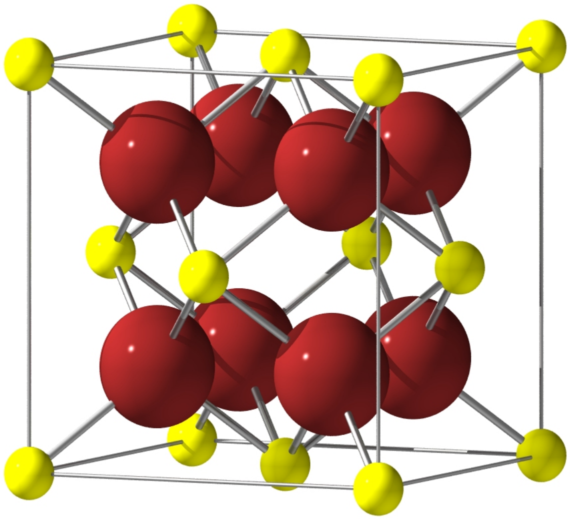

Figure 1.2: Unit cell of fluorite. The yellow atoms represent 4+ cations and the red atoms represent 2- anions.

It should be noted that there are exceptions to Pauling's first rule, as it is solely based on simple geometry. Firstly, if the anions are smaller than the cations (as is the case for the anti-fluorite structures Li_2O, Na_2O and K_2O), then the anion - cation radius ratio must be used (as opposed to the cation - anion). Other exceptions, including UO_2, occur because this rule assumes ions to be rigid spheres, which of course they are not. Partial covalency also contributes to further exceptions. Although Pauling's first rule is useful when making simple predictions, it is clear that more rigorous techniques, such as atomistic simulation, are required in order to generate more accurate predictions.

1.1.2 $A_2B_2O_7$ Pyrochlore Oxides

Pyrochlore oxides are named after the mineral pyrochlore, (NaCa)(NbTa)O_6F/(OH), with which they share a similar structure [10]. $A_2B_2O_7$ pyrochlores are ternary metallic oxides whose crystal chemistry is complex enough to make them favourable for a wide range of applications. In this thesis, A and B cations are only considered as having charges of 3+ and 4+ respectively. However, there is another entire series of pyrochlore compounds consisting of 2+ and 5+ cations.

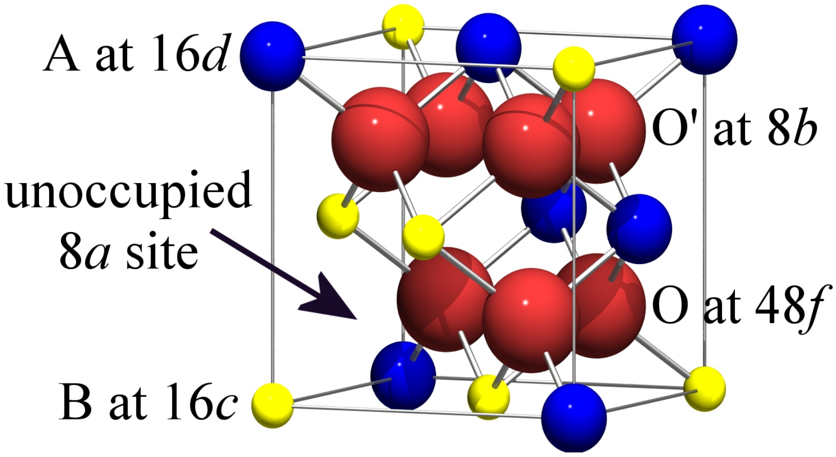

Figure 1.3: Unit cell of pyrochlore. Blue spheres represent A^{3+} cations, yellow B^{4+} and red O^{2-}.

The general formula of the oxide pyrochlore structure can be written as $A_2B_2O_6O'$. There are four crystallographically unique atom positions and the space group is *Fd3m* [10]. A common way of describing the structure is by fixing its origin on the B site, with atoms located at the following positions (using Wyckoff notation): A at 16*d*, B at 16*c*, O at 48*f* and O' at 8*b* [10]. The only internal positional variable of the pyrochlore structure is the oxygen x parameter, which characterizes the 48*f* oxygen atoms. To better visualize the pyrochlore structure, the convenient, fluorite type description is used [11, 12], see Figure 1.3. The pyrochlore structure can thereby be considered as an ordered, defective fluorite solid solution. In CaF_2, the fluorine anions are located in the tetrahedral sites of a Ca face centered cubic array. In this description of pyrochlore, the A and B cations form the face centered cubic array, but are additionally ordered in the <110> directions such that the A cations are eight coordinate and the B cations are six coordinate with respect to oxygen. This cation ordering means that the tetrahedral anion sites are no longer crystallographically identical. In fact, there are now three distinct tetrahedral sites: the 48*f*, which has two A and two B nearest neighbours, the 8*a*, which has four B nearest neighbours and the 8*b*, which has four A nearest neighbours. In pyrochlore, the 8*a* positions are vacant. Figure 1.3 depicts one eighth of the pyrochlore unit cell, which is analogous to a single fluorite unit cell. Figure 1.4 depicts a full unit cell of a pyrochlore, with the anions removed in order to better view the two cationic sublattices and the ordering along <110> directions.

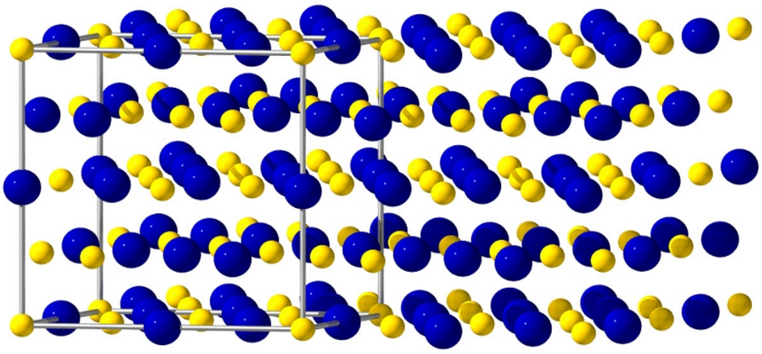

Figure 1.4: The cationic sublattice of pyrochlore.

1.2 Point Defects

All of the topics addressed in this thesis are concerned with deviations from the perfect periodic lattice. Though there are many ways in which crystal imperfections are manifest, such as dislocations, surfaces and pores, all of these are essentially conglomerations of zero dimensional point defects. Point defects consist of vacant lattice sites, atoms in non-regular lattice positions (so called *"interstitials,"* a term first coined by Wagner [13]) as well as impurity atoms. Many properties (e.g. conductivity, luminescence and diffusion) are influenced by the existence of these defects, which is particularly true for inorganic solids. Furthermore, it is not possible to produce a single crystal free of defects. Finally, as temperature increases, defects become even more important.

In this section, the different types of point defect and their means of creation are discussed. Kröger - Vink notation is used throughout [14].

1.2.1 Intrinsic Disorder

Intrinsic disorder is so termed because it requires only thermal activation, rather than the addition of impurities or solutes. As temperature is raised, contributions to the free energy due to the entropy term (increasing the magnitude of lattice vibrations and configurational terms) increase the number of atoms that are displaced from regular lattice positions. However, the concentration of defects is able to remain finite. This is because an increase in thermal energy also gives rise to an increase in entropy, thus reducing the free energy, which is evident in the following equation:

$$G = G^o + n \cdot \Delta g - T \cdot \Delta S_c \tag{1.1}$$

where ΔS_c is the configurational entropy due to the solution of defects, $n{\cdot}\Delta g$ is the free energy change necessary to create n interstitials and G^o is the free energy of a perfect crystal. The two most common types of crystalline defects in ionic materials are Frenkel [15] and Schottky defects [16, 17]. (It should be noted that thermodynamic equilibrium is not always reached, and therefore real materials contain a variety of defects due to slow kinetics of removal [18]).

Frenkel disorder results when an atom is displaced from its regular site to an interstitial site, thus forming a defect pair (see Figure 1.5). For a binary metal oxide MeO, the corresponding defect formation reaction is:

$$Me^x_{Me} + V^x_I \leftrightarrows Me^{\cdot\cdot}_I + V''_{Me} \tag{1.2}$$

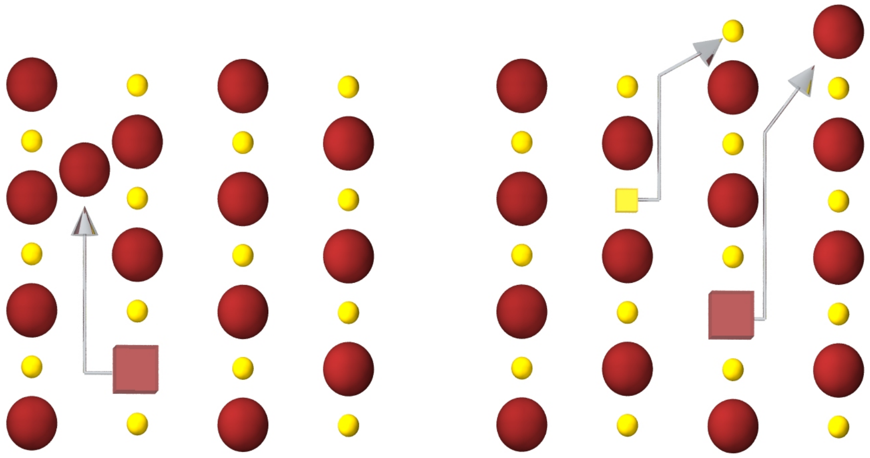

Figure 1.5: The left figure is Frenkel disorder in an ionic crystal, where the red square denotes a vacancy left by a cation which has moved to an interstitial site. The right figure is Schottky disorder.

Several compounds readily exhibit Frenkel disorder. For example, UO_2, CaF_2 and CeO_2, all demonstrate the Frenkel anion type of disorder (i.e. anion interstitials and anion vacancies) while AgCl, AgBr and Fe_3O_4 all exhibit cation Frenkel disorder. In this defect process, disorder, structural energy as well as entropy are increased. It is important to understand the factors which determine the concentrations of these types of defects. Recalling Equation 1.1, the configurational entropy can be expressed as:

$$\Delta S_c = k \cdot \ln \Omega \tag{1.3}$$

where Ω is the number of ways in which to arrange the defects in the crystal and k is Boltzmann's constant, leaving only a value for Ω, which can be expressed as:

$$\Omega_v = \frac{N!}{(N - n_v)! \cdot n_v!} \tag{1.4}$$

where Ω_v is the number of ways to arrange vacancies, N is the number of regular sites, and n_v is the number of vacancies. Similarly for interstitials:

$$\Omega_i = \frac{N!}{(N-n_i)! \cdot n_i!} \tag{1.5}$$

These equations can then be inserted into Equation 1.3, leading to:

$$\Delta S_c = k \cdot \ln \left\{ \left[\frac{N!}{(N-n_i)! \cdot n_i!} \right] \cdot \left[\frac{N!}{(N-n_v)! \cdot n_v!} \right] \right\} \tag{1.6}$$

Using the equality $n_i = n_v$ (for ceramics, this is the electroneutrality equation):

$$\Delta S_c = k \cdot \{\ 2\ln N! - 2\ln\left[(N-n)! \cdot n!\right]\} \tag{1.7}$$

If Stirling's approximation for large numbers [19] is employed:

$$\ln n! \approx n \ln n - n \tag{1.8}$$

then the expression for ΔS_c can be rewritten as:

$$\Delta S_c = 2k \cdot \{\ N\ln N - (N-n) \cdot \ln(N-n) - n \cdot \ln n\} \tag{1.9}$$

Equation 1.9 can be substituted into the equation for the free energy:

$$G = G^o + n \cdot \Delta g - 2kT \cdot \left\{\ N\ln\left[\frac{N}{N-n}\right] + n \cdot \ln \cdot \left[\frac{N-n}{n}\right]\right\} \tag{1.10}$$

At thermodynamic equilibrium, the free energy has a minimum with respect to n, i.e. $\left(\frac{\partial G}{\partial n}\right)_{T,P} = 0$. The expression for $\left(\frac{\partial G}{\partial n}\right)_{T,P}$ is obtained by differentiating Equation 1.10. If this is subject to the approximations for large N and small (i.e. dilute) concentration of defects, $N \gg n$, such that $N - n \approx N$, it is then possible to obtain [5]:

$$\frac{n}{N} = \exp\left(-\frac{\Delta g}{2kT}\right) = \exp\left(\frac{\Delta s}{2k}\right) \cdot \exp\left(-\frac{\Delta h}{2kT}\right) \tag{1.11}$$

It should also be noted that Δs is the entropic term which results from lattice strains and vibration frequencies altered by the presence of the defect. It is often the case that this term is assumed to be zero, despite the fact that values between 10^{-4} to 10^4 have been reported [5]. It is clear then that absolute defect concentrations are difficult to obtain with any degree of accuracy. Much more useful are the *relative* differences in defect concentrations (and indeed most defect related properties) between compounds.

The other type of intrinsic disorder previously mentioned is that of Schottky disorder [16, 17]. Schottky disorder is the simultaneous occurrence of cation and anion vacancies in thermal equilibrium, see Figure 1.5. In this case, vacancy defects must be formed in a number which maintains the electroneutrality of the lattice. For example, MgO forms both one magnesium and one oxygen vacancy (a Schottky pair) while TiO_2 forms a titanium vacancy and *two* oxygen vacancies:

$$Mg_{Mg}^{x} + O_{O}^{x} \leftrightarrows V_{Mg}'' + V_{O}^{\cdot\cdot} + MgO \tag{1.12}$$

and:

$$Ti_{Ti}^{x} + O_{O}^{x} \leftrightarrows V_{Ti}'''' + 2\ V_{O}^{\cdot\cdot} + TiO_2 \tag{1.13}$$

The thermodynamics are analogous to that of Frenkel disorder, see Equation 1.11, and the concentration of defects increases exponentially with temperature (i.e. $e^{-1/T}$).

Another type of intrinsic disorder that may exist is that of ionic interchange known as antisite disorder, where ions swap sites. This may seem unlikely, especially in particularly strong ionic, binary crystals [20], but as will be seen later, in materials with more than one cationic sublattice, swapping of cations is quite common indeed. It is also usual for all of these disorder processes to be present simultaneously, though one type of disorder typically predominates. In general terms, Frenkel disorder is more likely when the anion and cation differ substantially in size and when the lattice polarization is pronounced, e.g. AgBr [20, 21]. When the anions and cations are of similar size (as is the case for NaCl) Schottky disorder is favoured. Crystallography also plays a critical role. In close packed materials, there is little lattice space to accommodate an interstitial ion. It follows that Frenkel disorder is not favoured in these materials. Conversely, in open structures, Frenkel disorder is more easily accommodated.

1.2.2 Extrinsic Disorder

For the purpose of this thesis, intrinsic disorder is differentiated from extrinsic disorder as follows: intrinsic disorder only encompasses thermally activated defect processes which occur within an otherwise perfect lattice where there is no reaction with the environment. This is certainly a topic for debate, but inevitably it is only a matter of semantics (as elucidated by Chiang *et al.* [5]). Therefore, according to this definition, extrinsic disorder includes defects resulting from oxidation or reduction, i.e. non-stoichiometry. Essentially, extrinsic disorder includes reaction with gaseous species from the environment that are constituents of the lattice in question and reaction with species from the environment that are not native to the lattice. In cases of large formation energies or low concentrations of intrinsic defects, extrinsic behaviour can play the determinant role.

The concept of *stoichiometry* (i.e. the constant and fixed ratio of elemental constituents of a chemical compound) dates back to Dalton's atomic hypothesis [22], and more so the Law of Definite Proportions, which was a product of this hypothesis. This law states that the constituent elements of any compound exist in distinct proportions. This law was the topic for heated debate between Proust, a proponent of the law, and his fellow Frenchman Berthollet, who suggested that the composition of solid compounds is by no means constant. Berthollet lost that debate (in as much as the theory of Definite Proportions became a law), but was vindicated many years later in a paper by Kurnakov, where it was found that the constituents of various intermetallics varied in composition [23]. Schottky and Wagner went on to suggest that all inorganic solids are inherently non-stoichiometric [16].

The non-stoichiometry of metal oxides can be subdivided into two categories with respect to exact stoichiometry: metal deficient or oxygen deficient. Non-stoichiometry is a direct result of point defects and the extent of non-stoichiometry is measured by the net concentration of these defects [21]. Just as the reactions for Frenkel and Schottky disorder were electronically neutral, the reactions for non-stoichiometry must also be kept neutral through the formation of complimentary point defects. In metal deficient oxides, if metal vacancies are formed, they are complimented by electronic defects on either remaining metal sites (increasing the valence state), on the oxygen site (lowering the charge) or by a delocalized charge. If the metal sublattice remains intact, the non-stoichiometry is facilitated by oxygen interstitial defects compensated by the electronic defects mentioned above. It follows that for the oxygen deficient analogue, metal interstitials or oxygen vacancies will be the predominant structural defects.

A perhaps more clear example of extrinsic disorder, but still technologically significant, is the presence of impurity defects which are non-native to the compound. For example, doping a material (thus generating defects) can have pronounced effects on a variety of properties: doping Si with group V atoms Sb, As, P or group III atoms In, Al or B creates charge carriers for n- and p- type semiconductors respectively [24]. In addition, the solution of $CaCl_2$ lowers the density of KCl with the production of K vacancies [25]. Finally, the cubic fluorite structure of ZrO_2 can be stabilized with a variety of oxides such as Y_2O_3 or CaO. The latter example is particularly important in electrochemical applications due to the generation of anion vacancies.

For example:

$$CaO_{(g)} + (Zr_{Zr})^{x} + (O_O)^{x} \leftrightarrows (Ca_{Zr})'' + (V_O)^{\cdot\cdot} + ZrO_2 \tag{1.14}$$

1.2.3 Fission Produced Defects

The impurity defects considered in this thesis are generated by the fission process (a term borrowed by Otto Frisch [26, 27] after learning from a biologist colleague, William Arnold, of the word for cell division [28]) and not through doping. Although the discovery of nuclear fission is relatively recent, because of its complexity and implications, much research has been done to further the understanding of this phenomenon. By 1936, Fermi and others [29–31] were able to show that slow neutrons were able to disintegrate nuclei. However, it was the strange manner in which uranium disintegrated which made it so exciting. Uranium is naturally radioactive and disintegrates via the emission of alpha particles. The fact that slow neutron irradiation was leading to beta ray emission meant that a different process was taking place. In 1939, Hahn and Strassman [32] found at least three radioactive bodies when bombarding uranium with neutrons, one of which was barium. Initially it had been believed that radium was being produced. This misconception was on account of the limitations of atomic theory at the time. After many thorough chemical experiments it became clear that the substance Hahn and Strassman obtained was barium, and thereby it was deduced that the uranium nucleus, after capturing a neutron is able to split into two nuclei (Niels Bohr stated after this discovery, “Oh, what fools we have been. We should have seen that before!” [28]). Although a detailed account of the fission process mechanism is not justifiable (and can be found elsewhere: see Fission, Chapter 10, by J.A. Wheeler and I.G. Schröder in [33]), a few points are relevant. The following reaction describes a typical example of the fission of U^{235} [34]:

$$ {}_on^1 +_{92} U^{235} \rightarrow_{92} U^{236*} \rightarrow_{57} La^{139} +_{42} Mo^{95} + 2_0n^1 \tag{1.15}$$

The total energy released by a fission event can be expressed as [35]:

$$\Delta E = (M_o - \Sigma M_i)c^2 \tag{1.16}$$

where M_o is the mass of the original nucleus (U^{235} in the example case) and M_i is the mass of the resulting nuclei ($2 \cdot M_{neutron} + La^{138.955} + Mo^{94.945}$). An energy of 200 MeV results from the mass change of 0.215 amu.

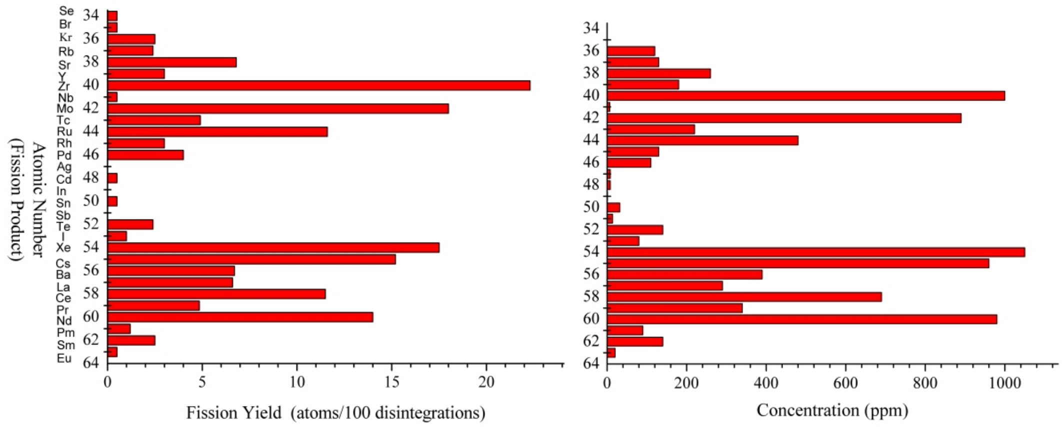

Figure 1.6: Fission product yield for a PWR fuel rod after 2.9% burnup, reproduced from [36] and after 1% burnup after data given in [37].

The fragments of the fission process quickly emit neutrons after the fission event because they are proton deficient. The fission products are left as a charge deficient pair and continue toward a stable state through β decay or via excited states. Though rare, uranium is also known to split into three and four fission products. The left hand plot in Figure 1.6 displays the number of each fission product resulting from the fission of 100 uranium atoms, while the right hand plot is the concentration of fission products in weight-ppm for a fuel pin with a different history. Although both sets of data originate from U-235 fuel, differing only in burnup percentage, there are some slight differences. However, in both plots, there is a very pronounced double peak for the statistical distribution of fission products. This double peak is strongly dependent on what has induced the fission event. The slower the neutrons, the more pronounced the peaks. Higher energy neutrons give rise to a more symmetrical curve. Another important fact that can be observed in Figure 1.6 is that there are a significant number of decay atoms present, each of which will behave in a different chemical and physical manner.

1.2.4 Association of Point Defects

As previously mentioned, it is possible, and in fact likely that different types of defects will exist. However, a model based upon the assumption that point defects form an ideal solution is too simple. An important behaviour to consider is the interaction between defects, especially those exhibiting Coulombic attraction due to their opposite charges. The interaction between defects is, among other things, a function of their concentration. At low concentrations, ideal solution defect models are useful, but as the concentration of defects increases, activity coefficients must be introduced. The first attempt to correct activity dependent defect interactions was the Debye - Hückel theory [38, 39], which was initially developed for aqueous, electrolytic solutions. The basis of this theory is that all deviations from ideal behaviour can be accounted for by electrostatic interaction between charged species. If one ion is considered, it can be thought of as attracting a cloud of oppositely charged ions, which screen it from all other defects, thereby decreasing the chemical potential. Chemical potential in this case can be expressed as an activity coefficient. The end result of the Debye - Hückel treatment is that the activity coefficient for any defect is less than its concentration. The mean activity coefficient, $f_{\pm}$, is expressed as:

$$f_{\pm} = exp\left\{ -\frac{e_o^2}{8\pi \cdot \epsilon_o \cdot \epsilon \cdot kT} \cdot \frac{b}{1 + b \cdot a} \cdot |z_+ \cdot z_-| \right\} \tag{1.17}$$

where e_o is the charge of an electron, ϵ is the relative dielectric constant (permittivity), ϵ_o is the absolute dielectric constant, k is Boltzmann's constant, a is the smallest distance after which associates will not form and z_+, z_- are the charges of the point defects considered. The distance, $\frac{1}{b}$, is known as the Debye length and can be expressed as:

$$b = \sqrt{\frac{e_o^2}{\epsilon_o \cdot \epsilon \cdot kT} \cdot \sum_i n_i \cdot z_i^2} \tag{1.18}$$

where n_i is the number of defect species per cm^3. From this equation, it is clear that the Debye length (the screening length) increases with a decrease in the defect concentration or an increase in the dielectric constant. Unfortunately, the Debye-Hückel correction is not necessarily realistic physically when applied to defective solids (after all, it was developed for liquids). Firstly, ϵ is a function of temperature and is generally unknown. What's more, the dielectric constant is a bulk value which is meaningless when applied to atomic distances. Thus, the Debye-Hückel theory is only valid at low defect concentrations.

The work described in this thesis is concerned with fluorite compounds which display very high defect concentrations such that close defect association is practically imposed. As such, a Debye-Hückel correction is not appropriate.[1] Rather, it is sufficient to simply consider defect associations explicitly at an atomic level (and therefore *defect clustering*). This relates our results to low temperatures but high defect concentrations; conditions which are generally satisfied by the compounds investigated in this study.

---

[1] More complex models have been developed to account for defect interactions (e.g. [40,41]), but these are not practical for this study.

1.3 Surfaces

A useful way of considering a surface, at least from the perspective of the ions directly beneath the surface, is as a giant defect [42] and the positions of these ions are relaxed as if they were responding to a point defect. The ultimate effect of this relaxation can be significant. In fact, many properties and phenomena of ionic crystals are governed by surfaces, such as mechanical strength, catalysis and crystal morphology. A convenient way of envisioning a surface is as a cleaved crystal consisting of stacked planes. According to Tasker [43], there are then three types of surface, as shown in Figure 1.7.

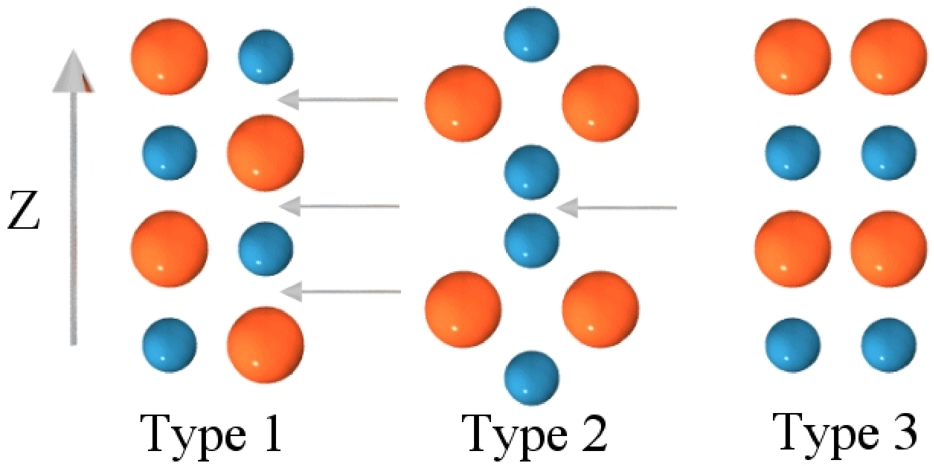

Figure 1.7: The types of ionic surface according to Tasker [43]. The horizontal arrows indicate planes along which the crystal can be cut without forming a dipole.

A Type 1 surface is a series of neutral planes, each plane consisting of a stoichiometric ratio of anions and cations. A Type 2 surface consists of charged planes, but arranged symmetrically such that there is no dipole moment perpendicular to the surface, so long as the surface is cut between neutral blocks. A Type 3 surface is a series of alternately charged planes, but however the crystal is oriented, it is not possible to form a surface free of a dipole moment. Chapter 4 is concerned with results for the segregation of fission products to low index surfaces of UO_2 and will discuss the structure of each of these surface types that form in fluorite in detail. As will be shown, each of these Tasker surface types is represented by the three low index surfaces of UO_2.

The stability of a surface is controlled by its *surface energy* which is defined as: [42]

$$\gamma = \frac{(E_{crystal\ with\ surface}) - (E_{bulk})}{(surface\ area)} \tag{1.19}$$

Surface energies are capable of being calculated (the details of which will be discussed in Section 2.3) providing information on surface stability [44] and thus for equilibrium crystal morphology [45–48]. It has been shown that if there exists a dipole perpendicular to the surface, the surface energy is infinite and such surfaces do not occur [49]. Recalling that Type 3 surfaces have such a dipole moment, it follows that they will not form unless the dipole is neutralized by defects. Typically, a number of ions must be removed from the surface and placed on the bottom of the crystal. This generates a dipole across the crystal that is in opposition to the surface dipole.

1.4 Transport

1.4.1 Diffusion Equations

Transport in ceramics, both mass and electrical, is an important and complicated phenomenon. For example, mass transport governs the densification process during sintering while electrical transport is necessary for fuel cells. Diffusion is the transport of matter, in the form of atoms, ions or molecules and is responsible for most structural changes. The common way of describing diffusion is through Fick's first law [50]:

$$J = -D\left(\frac{dC}{dx}\right) \tag{1.20}$$

where J is the flux of a species in moles per unit area time unit (e.g. mol/(cm^2· sec)), D is the *diffusion coefficient* and dC/dx is a concentration gradient. D is a useful property of materials, since it describes the rate of diffusion of a species, or its *diffusivity* and usually appears in units of cm^2/sec. Fick's first law is analogous to both Ohm's law for electrical conduction and Fourier's law of heat conduction [51] (though it should be pointed out that these are not actually "laws," but rather mathematical descriptions of phenomena). Fick's first law is applicable in steady state situations, when J is independent of time. However, if the concentration, C, varies with time (i.e. non-steady state), then Fick's first law becomes more difficult to use. The increase in concentration with time must equal the negative flux:

$$\frac{\partial C}{\partial t} = -\frac{\partial J}{\partial x} \tag{1.21}$$

and then substituting Fick's first law, to obtain:

$$\frac{\partial C}{\partial t} = -D\frac{\partial^2 C}{\partial x^2} \tag{1.22}$$

which is commonly known as Fick's second law. Solutions to Fick's second law become very complicated, often involving error functions, infinite trigonometric series as well as Bessel functions (common in cylindrical geometries). In depth discussions of Fick's second law and its solutions can be found elsewhere [52, 53].

1.4.2 Atomistic Theory of Diffusion

This account of diffusion has thus far been strictly phenomenological, and has not yet addressed the atomistic theory of diffusion. Diffusion on the microscopic scale was first documented by Robert Brown after having observed the seemingly random movement of pollen particles immersed in water [54]:

> *These motions were such as to satisfy me, after frequently repeated observation, that they arose neither from currents in the fluid, nor from its gradual evaporation, but belonged to the particle itself.*

Initially, Brown thought this "movement" to be a characteristic of only organic substances, referring to them as "*elementary active particles*," but eventually included inorganic material as well after further experimentation (even having tested powder obtained from a fragment of the Sphinx). Such was the lack of understanding, that Brown cautiously warned:

> *The dust or soot deposited on all bodies in such quantity, especially in London, is entirely composed of these molecules.*

Despite continuous research on so called Brownian motion, it was not until the early 20^{th} century that Smoluchowski [55] and Einstein [56, 57] provided a precise explanation. This problem, commonly referred to as "random-walk," attempts to determine the final position of particles by using jump frequencies and average jump distances. If a block of material is considered as having a concentration gradient along its x axis (see Figure 1.8), an equation can be derived which relates D to the jump frequency and jump distance.

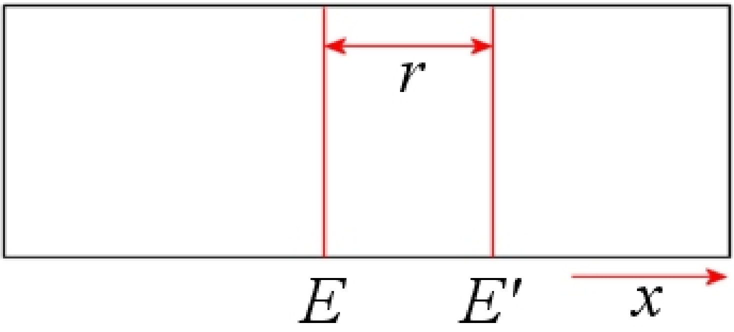

Figure 1.8: A bar with a concentration gradient in the x direction, after [58].

Assume two planes, E and E', are separated by a distance r. If there are n_1 atoms diffusing per unit area in plane E and n_2 atoms diffusing per unit area in plane E', and if the average jump frequency is Γ, it follows that the net flux is:

$$J = \frac{1}{6}\,(n_1 - n_2)\Gamma = \frac{(number\ of\ atoms)}{(area)(time)} \tag{1.23}$$

Concentrations c_1 and c_2 can be written as:

$$\frac{n_1}{r} = c_1 \quad \text{and} \quad \frac{n_2}{r} = c_2 \tag{1.24}$$

This can then be substituted into Equation 1.23:

$$J = \frac{1}{6}\,(c_1 - c_2)r \cdot \Gamma \tag{1.25}$$

Generally, concentration changes are slow enough that they can be expressed as [52]:

$$c_1 - c_2 = -r\left(\frac{\partial c}{\partial x}\right) \tag{1.26}$$

Which is essentially Fick's first law, if the diffusion constant is expressed as:

$$D = \frac{1}{6}\,\Gamma \cdot r^2 \tag{1.27}$$

Equation 1.27 is the definition of the diffusion coefficient in solid state systems. It consists of a geometric factor ($= \frac{1}{6}$ in this case because of the six directions in space which an atom can jump), an elementary jump distance squared (= r^2 which is proportional to the lattice parameter) and an effective jump frequency (= Γ).[2] (A more detailed discussion of random walk and the diffusion coefficient becomes rather complicated and is not warranted by this thesis and can be found elsewhere [52,61].)

There are several possible mechanisms for the diffusion of ions and atoms, those of which are predominant in the crystalline solids are now described. The *interstitial mechanism* is the diffusion of an atom via interstices, see Figure 1.9.

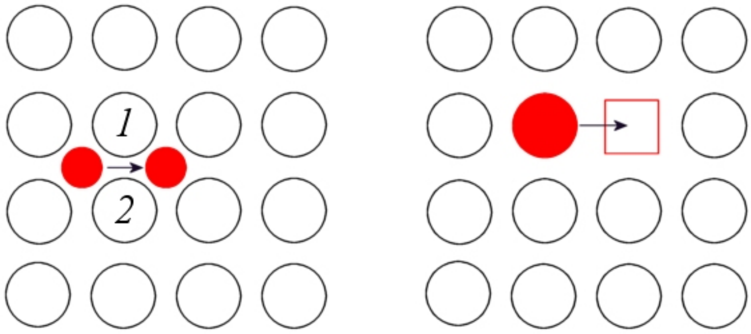

Figure 1.9: The interstitial and vacancy diffusion mechanisms.

An obvious prerequisite of this type of diffusion is that there are defects residing in interstitial positions. This mechanism is most likely to occur with small solutes, as there is a local deformation of the lattice. In Figure 1.9, where atoms labelled 1 and 2 must move in order for the interstitial atom to move into its new position. Another type of diffusion mechanism is known as the *vacancy mechanism*. In this case, adjacent atoms are able to jump into these unoccupied sites (denoted by the square in Figure 1.9). There is much less distortion to the lattice when atoms diffuse via this mechanism compared to diffusion via the interstitial mechanism.

---

[2] An interesting aside is that Perrin used Einstein's kinetic theory of random walk to determine Avogadro's number [59,60].

Due to the severe lattice distortions required, larger atoms occupying interstitial sites are unable to diffuse via an interstitial mechanism. However, an alternative is afforded by the *interstitialcy mechanism*, in which an interstitial atom forces an adjacent atom on a regular lattice site into an interstitial site, see Figure 1.10.

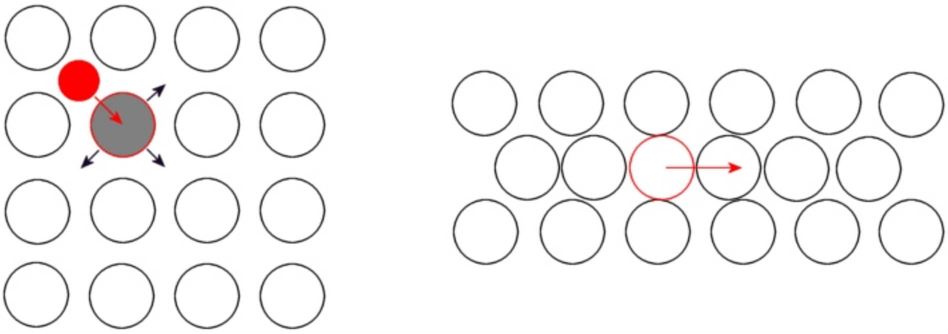

Figure 1.10: The interstitialcy and crowdion diffusion mechanisms.

This type of diffusion can be collinear (if the displaced atom moves in the direction of the red arrow in Figure 1.10) or non-collinear (if it moves in other directions than the red arrow). A related diffusion mechanism occurs when an interstitial occurs in a close packed direction, and is known as the *crowdion mechanism*. The extra atom in the row displaces several atoms from their regular sites, see Figure 1.10. Although this mechanism is not likely for ionic materials because of the strong Coulombic forces involved, it may be important after irradiation, especially in metals.

It has already been stated that it is not unlikely for several types of defects to be present simultaneously. Each of the diffusion mechanisms discussed is dependent on point defects. Therefore, several types of diffusion mechanism can co-exist, with one generally predominating. It follows that diffusion is directly related to the concentration of defects and their mobility.

1.4.3 Segregation

The *segregation* of fission products to surfaces of UO_2 is discussed in Chapter 4, where segregation is the movement of a species toward (or away from) a surface, boundary or interface. Theoretical explanations for surface segregation date back to Gibbs [62], and his description of a *dividing surface* between two bulk phases. Despite the fairly long time of qualitative understanding, it is only recently that analytical instruments have been developed to feasibly investigate this phenomenon (e.g. Auger electron spectroscopy [63]). Nevertheless, segregation trends are difficult to extract from experimental data. This can be attributed to the complexity of segregation. Factors such as ionic space charge, the compensation of surface charge beneath the surface, and surface strain effects further complicate the segregation phenomenon. Chapter 4 discusses yet more complications encountered during this work.